BULLETIN OF THE POLISH ACADEMY OF SCIENCES
TECHNICAL SCIENCES,
DOI: 10.24425/bpasts.2025.153230

Calibration by Diffeomorphisms of Robot Manipulator Kinematics: a Novel Approach

Roberto Orozco[1]* **Adam Ratajczak**[2]

[1] Faculty of Electronics, Photonics and Microsystems, Wrocław University of Science and Technology, Poland
[2] Faculty of Information and Communication Technology, Wrocław University of Science and Technology, Poland

Abstract. Our paper presents a nonparametric data-driven technique that can enhance the accuracy of robot kinematics models by reducing geometric and nongeometric inaccuracies. We propose this approach based on the theory of singular maps and the Large Dense Diffeomorphic Metric Mapping (LDDMM) framework, which has been developed in the field of Computational Anatomy. This framework can be thought of as a method for identifying nonlinear static models that encode a priori knowledge as a nominal model that we deform using diffeomorphisms. To tackle the kinematic calibration problem, we implement Calibration by Diffeomorphisms and obtain a solution using an image registration formalism. We evaluate our approach via simulations on double pendulum robot models, which account for both geometric and nongeometric discrepancies. The simulations demonstrate an improvement in the precision of the kinematics results for both types of inaccuracies. Additionally, we discuss the potential application of physical experiments. Our approach provides a fresh perspective on robot kinematics calibration using Calibration by Diffeomorphisms, and it has the potential to address inaccuracies caused by unknown or difficult-to-model phenomena.

Key words: kinematics, robot kinematics calibration, diffeomorphisms, Calibration by Diffeomorphisms

1. INTRODUCTION

The robotic manipulators' repeatability, accuracy and precision are the features that give them a raison detre in the industrial realm. The main factor for robots being precise and accurate is the correctness of their mathematical model of kinematics embedded in the controllers software. These models usually rely on common modelling methods, such as the Denavit-Hartenberg or the Product of Exponentials method, covering standard serial robot geometries. As it may be expected, the kinematics model of the actual robot usually differs from the one created in the design, thus affecting the precision and accuracy. This drives one to enhance the nominal kinematics.

According to the literature [1], the process of refinement of the performance of the kinematics model is referred to as a robot kinematics calibration problem. The problem may be described as follows. Having a real robot and the ability to perform some measurements on it, propose a reformulation of the known nominal kinematics that will be closer to the actual kinematics in some predefined criterion.

In general, the robot kinematics is represented as a map $k\colon X \times P \longrightarrow Y$ having the admissible joints position $x \in X$ and model parameters $p \in P$ as arguments, taking the pose of the end-effector as values $y \in Y$. A typical set of parameters is the one that follows the Denavit-Hartenberg algorithm and governs the geometry of the robot, although it is not the only possible one. Simply speaking, the set of parameters may be broader depending on the details of the modelling process.

Following [2, 3], it can be seen that the most significant step of the robot kinematics calibration is the one that employs model identification algorithms. A widely spread approach is the so-called parametric calibration. The idea behind it relies on looking for a new set of model parameters better describing the robot's kinematics. The standard procedure exploits the measurements (x_i, y_i) of the joints' position and corresponding end-effector poses to obtain finer values of the parameters p, minimising the mean squared error. Despite good theoretical and practical results, such an approach has its drawbacks. Specifically speaking, for exact calibration, the method requires knowledge of the complete model of the robot kinematics (structures, formulas etc.), which in practice is difficult to achieve.

Discrepancies appearing in robot models may be grouped into: geometric and non-geometric inaccuracies. The first one is sourced in the variations of geometric parameters, while the second one is caused by phenomena that are unknown or hard to model, e.g. a joint compliance, with the last one seeming to be an unbreakable wall for a parametric approach. Usually, in such a case non-parmetric approaches are used in model identification. To the best knowledge of the authors, aside from employing neural networks [4, 5, 6, 7], the non-parametric approaches did not bring enough attention to the robotic society.

An alternative approach and possible remedy for the mentioned pitfalls is to restate the calibration problem in a different mathematical framework requiring milder assumptions. Such an attempt has been made in the paper [8], developing so-called Calibration by Diffeomorphisms. That work set the problem of robot calibration in terms of the differential equivalence of the singular maps. Despite fruitful theoretical results, the paper lacks a practical implementation of the findings due to difficulties in computing diffeomorphisms. Currently, the development of computational methods for diffeomorphic transformations in Computational Anatomy unveils new opportunities for revisiting the approach proposed in [8] that allows us to design a data-driven method for robot calibration problems alternative to machine learning. Indeed, the presented method is an alternative to classical Machine Learning, but nevertheless it can also be considered as a type of learning process. Based on the collected measurements (data-driven), we iteratively propose

*e-mail: roberto.orozco@pwr.edu.pl

new and better kinematics (learning). In contrast to Machine Learning, our process converges to an optimal solution in a known number of iterations. Finally, the results can be easily generalised to areas not covered by the measurements.

The robot calibration problem is known in the robotic literature and has been extensively studied since the end of the last century [2, 9, 10]. Nowadays, this topic is an attractive and meaningful research field – a relatively large number of appearing scientific papers are devoted to the calibration of industrial robots [11, 12, 13, 14, 15, 16, 17], and investigations in other applications appear, for example, in the calibration of the surgical robots, [18]. In [19, 20], the so-called elasto-geometrical calibration method has been introduced. According to [21], it is necessary to use a two-step method to address the differences between the end-effector position and orientation discrepancies. In the study [22], the authors delved even deeper into the calibration process and analysed the uncertainty of its results. They were able to determine how parameter uncertainty affects position uncertainty. These findings may provide suggestions for optimal measurement conditions. In reference [23], the authors employ the formula for the Product of the Exponentials instead of the traditional Denavit-Hartenberg algorithm for modelling the kinematics. It was done to leverage the modelling method's benefits in the calibration process. The introduction of Finite and Instantaneous Screw Theory allows the authors of [24] to define the unique calibration method for serial and parallel manipulators. Finally, other research is focused on the measurement aspects of calibration. Laser trackers, optical CMMs (Coordinate Measuring Machines), or single and multiple cameras are typically considered [25].

Our research is focused on the fundamentals of the calibration problem. We introduce a new and distinct data-driven approach to kinematics calibration that in fact may be used for objects different than robot kinematics. It might be seen as method for identification nonlinear static model in which the apriori knowledge is encoded as 'nominal model' that we would like to deform by diffeomorphisms. In terms of block-structured systems proposed calibration model is similar to Wiener-Hammerstein models, but all of the blocks are (possibly) nonlinear, the central block is the one we incorporate the appriori knowledge (nominal model) and the first and last are diffeomorphisms. At this stage of research, we do not provide physical experiments. The goal is to develop a computational framework for calibration by diffeomorphisms making further experiments on the robots possible. Some preliminary research was recently published locally in [26].

After the introductory words, we state the main contribution of this paper, which is threefold:

1. discussion about the idea of Calibration by Diffeomorphisms, [8], and necessary modifications for numerical implementation.
2. introduction of a novel, data-driven, non-parametric kinematics calibration algorithm, drawing upon the Calibration by Diffeomorphisms concept.
3. a fusion of the numerical algorithms from the Computational Anatomy, [27], with the Calibration by Diffeomorphisms methodology.

The composition of this paper is as follows. The next section, 2, recalls theoretical fundamentals and results of the Calibration by Diffeomorphisms. Afterwards in section 3, the problem of robot kinematics calibration by diffeomorphisms is restated in terms of Large Deformation Diffeomorphic Mapping (LDDMM) framework. The implementational details have been derived in section 4. Section 5 evaluates the theoretical results through simulation for calibration of a double pendulum (an *RR* manipulator) with both geometric and non-geometric inaccuracies. Finally, the discussion of the results concludes the paper with section 6.

2. CALIBRATION BY DIFFEOMORPHISMS

The Calibration by Diffeomorphisms mentioned above has been proposed in [8] as a theoretical framework for solving the kinematic calibration problem. As the author points out, the motive for the work was to set the theoretical fundamentals for a rather practical problem that would allow one to answer whether or not a correction for a given kinematics model could be computed. That aim drove him to settle the calibration problem in terms of the singularity theory (theory of stable mappings).

Before we introduce the main concepts of Calibration by Diffeomorphisms we shall consider the objects of our interests and define the kinematics calibration problem. A general n-degree-of-freedom rigid manipulator consists of r unlimited revolute joints and the $n-r$ prismatic joints. The internal/joint space X of such a manipulator may be identified with a smooth manifold $X = R^{n-r} \times T^r$, where T^r denotes $r-$dimensional torus. This space (manifold) may be interpreted as the space of the admissible joint positions. The standard way of representing manipulator kinematics is to assign for each joint position (element of X) a pose of the manipulator's end-effector (position and orientation expressed in a coordinate frame of a manipulator's fixed base). The external space Y of admissible poses is a smooth manifold and subgroup of the $SE(3)$ Lie group. Having defined the internal and external space, we can describe the kinematics as a smooth map

$$k\colon X \to Y.$$

If we fix the internal and external spaces, k may be considered as an element of $C^\infty(X,Y)$ – the set of smooth mappings between those manifolds. Finally, with the kinematics mapping defined, the calibration problem can be stated as follows, given nominal kinematics k, find a calibrating transformations that applied to k would produce the actual kinematics k', with $k,k' \in C^\infty(X,Y)$.

The calibration by diffeomorphism exploits two concepts of singularity theory: LR-equivalence and structural stability [28]. The first one states that two maps $k,k' \in C^\infty(X,Y)$ are equivalent if there exist diffeomorphisms $\varphi \in \mathrm{Diff}(X)$ and $\psi \in \mathrm{Diff}(Y)$ that $\psi \circ k \circ \varphi^{-1} = k'$. The latter one yields that a smooth map k is structurally stable if any k' in the neighbourhood of k is LR-equivalent to k. Let us denote k as nominal

kinematics – the known one, and defined by the model and k' as actual kinematics – the real, unknown one. Then according to [8] we can restate the robot kinematics calibration problem in terms of Calibration by Diffeomorphisms.

Let nominal kinematics k and actual kinematics k' be smooth maps, i.e $k,k' \in C^\infty(X,Y)$, then k can be calibrated to k' if there exists calibrating transformations $\varphi \in \mathrm{Diff}(X)$ and $\psi \in \mathrm{Diff}(Y)$ such that

$$\psi \circ k \circ \varphi^{-1} = k',$$

It can be seen that the definition of calibration by diffeomorphism follows directly from the LR-equivalence. Let us look closely at the two diffeomorphisms acting on the appropriate spaces. If we slightly abuse the notation, then $\varphi\colon X \longrightarrow X'$ and $\psi\colon Y \longrightarrow Y'$, where X' and Y' denote the diffeomorphically transformed spaces. They retain the nominal topology but obviously can change the geometry. We are now ready to compose the following commutative diagram

$$\begin{array}{ccc} X & \xrightarrow{\;k\;} & Y \\ \downarrow{\scriptstyle \varphi} & & \downarrow{\scriptstyle \psi}\,. \\ X' & \xrightarrow{\;k'\;} & Y' \end{array} \tag{1}$$

As we can see, the idea behind this is to deform the domain and the image of the nominal kinematics so that the resulting one aligns with the kinematics of the real robot.

Nevertheless, one would like to know whether such calibrating transformation exists. The answer to this question follows directly from the property of structural stability, i.e., the calibrating transformations exist for structurally stable nominal kinematics. Several classes of structurally stable maps have been discovered in the theory of stable mappings. The work [8] presents some of the results and adapts them to the scope of kinematics calibration.

Tchoń in [8] introduces a method for computing so-called affine calibrating transformations yielding explicit expressions for the diffeomorphisms. This approach assumes that the nominal kinematics k is subject exclusively to small parametric variations u ($u \in R^s$ being a variation of the model parameters $p \in R^s$), and the diffeomorphisms can be expressed affine in u, i.e., $\psi(y) = y + \frac{\partial \psi(y)}{\partial y}\big|_{u=0} u$, $\varphi(x) = x + \frac{\partial \varphi(x)}{\partial x}\big|_{u=0} u$.

In this paper, we consider the problem of calibration by diffeomorphism without constraining ourselves to small discrepancies of the model and affine form of the diffeomorphisms. The methodology for that case follows directly from homotopic stability [28] that states: for proper nominal kinematics k, there exists a one-dimensional family, parametrized by $\vartheta \in R$ of calibrating transformations $\varphi_\vartheta \in \mathrm{Diff}(X)$ and $\psi_\vartheta \in \mathrm{Diff}(Y)$ with $\varphi_0 = \varphi_\vartheta|_{\vartheta=0} = \mathrm{id}_X$, $\psi_0 = \psi_\vartheta|_{\vartheta=0} = \mathrm{id}_Y$, such that actual kinematics k_ϑ takes the form

$$k_\vartheta(x) = \psi_\vartheta \circ k \circ \varphi_\vartheta^{-1}(x). \tag{2}$$

It states the existence of a one-parameter family of calibrating transformations depending on the parameter $\vartheta \in R$ and is the entry-point of our deliberation. Unfortunately, it says barely anything about how to compute the calibrating diffeomorphisms. However, similar problems have been widely studied in the past decades, for example, in Computational Anatomy [27, 29]. One of its results is the so-called Large Deformation Diffeomorphic Metric Mapping framework that allows one to solve the image registration problem [27]. An adaptation of its brilliant mathematical machinery we introduce in the subsequent section.

3. MAIN RESULT

Relying on the unified abstract framework originally devoted to image registration, we may formally address the main problem of robot calibration. Let us define the space of objects V, on which a group of diffeomorphisms will act, as the space $C^\infty(X,Y)$ of smooth mappings between the internal space X and the external space Y. Since we are addressing the problem of calibrating the robot's kinematics, and kinematics is inherently a smooth mapping between X and Y, we will consider the space V to consist of such kinematic mappings. Thus, we will denote it as a space of kinematics. In this setting, we constrain ourselves to the robot kinematics that may be expressed in coordinates, i.e., $Y = R^m$. We identify configuration space with n-dimensional Euclidean space $X = R^n$, so a kinematics is a map

$$k\colon X \simeq R^n \longrightarrow Y \simeq R^m, \tag{3}$$

and seemingly $k \in V \simeq C^\infty(R^n,R^m)$. On the other hand, to be consistent with the calibration by diffeomorphisms, we shall set the group of transformation G to be $G = \mathrm{Diff}(X) \times \mathrm{Diff}(Y) \simeq \mathrm{Diff}(R^n) \times \mathrm{Diff}(R^m)$. Unfortunately, we have to take a different approach due to numerical implementation issues. Instead of dealing with a whole group G, we shall stick to a subgroup that arises as a flow of appropriate ordinary differential equations (ODEs). It is done by considering a group of diffeomorphisms emerging from the admissible space of vector fields. The broadly described details can be found in [29]. The procedure of building such groups boils down to the choice of the space of vector fields $\mathscr{V}$ that is admissible (continuously embedded in $C_0^1\left(R^d,R^d\right)$, continuously differentiable vector fields on R^d that tend to 0 at infinity), then the group of diffeomorphisms $\mathrm{Diff}_\mathscr{V}$ is the set of diffeomorphisms being flows from time 0 to 1 of the vector fields from that space. In this case elements of $\mathrm{Diff}_\mathscr{V}$ inherit smoothness properties from $\mathscr{V}$. Thus, we shall choose the space H^∞ – intersection of all Sobolev space. Finally, we get $G = \mathrm{Diff}_\mathscr{V}(X) \times \mathrm{Diff}_\mathscr{W}(Y)$ consisting of diffeomorphisms emerging as a flow of the vector fields living in the product space $\mathscr{V} \times \mathscr{W} \simeq H^\infty(X,R^n) \times H^\infty(Y,R^m)$, i.e.

$$\begin{cases} \frac{\partial \varphi_\vartheta}{\partial \vartheta} = v_\vartheta(\varphi_\vartheta), & \varphi_0 = \mathrm{id}_X, \\ \frac{\partial \psi_\vartheta}{\partial \vartheta} = w_\vartheta(\psi_\vartheta), & \psi_0 = \mathrm{id}_Y, \end{cases} \tag{4}$$

for $g_\vartheta = (\varphi_\vartheta, \psi_\vartheta) \in G$ and $u_\vartheta = (v_\vartheta, w_\vartheta) \in \mathscr{V} \times \mathscr{W}$.

Having specified the group G, we may discuss the action of G on V. It is defined in the following way. Let $g = (\varphi, \psi)$, $g \in G$, and $k \in V$ then $g \cdot k = \psi \circ k \circ \varphi^{-1}$. It is easy to check that the action is a left action. Finally, we can formulate

the calibration by diffeomorphisms problem in the LDDMM framework [29]. In that terms the calibration problem substantiate as a variational optimization problem

$$\min_u E(u) = \frac{1}{2}\int_0^1 \|u_\vartheta\|^2_{\mathscr{V}\times\mathscr{W}}\,\mathrm{d}\vartheta + \frac{1}{2\sigma^2}\|g_1\cdot k_0 - k\|^2_V, \quad (5)$$

subject to

$$\frac{\partial g_\vartheta}{\partial\vartheta} = u_\vartheta\cdot g_\vartheta, \quad g_0 = e, \quad (6)$$

where $u_\vartheta = (v_\vartheta, w_\vartheta)\in\mathscr{V}\times\mathscr{W}$, $u_\vartheta\cdot g_\vartheta = (v_\vartheta(\varphi_\vartheta), w_\vartheta(\psi_\vartheta))$ and $g_1 = (\varphi_1,\psi_1)\in G$ is the endpoint map of the differential equation above. The norm in the functional (5) are induced from the inner products. The first one takes the form

$$\langle u_1,u_2\rangle_{\mathscr{V}\times\mathscr{W}} = \langle v_1,v_2\rangle_{\mathscr{V}} + \langle w_1,w_2\rangle_{\mathscr{W}}, \quad (7)$$

where $u_i = (v_i,w_i)\in\mathscr{V}\times\mathscr{W}$ and the inner products on the right hand side are the inner products for the appropriate admissible vector space, i.e.,

$$\langle v_1,v_2\rangle_{\mathscr{V}} = \int_{R^n} v_1^\top(x)L_{\mathscr{V}}v_2(x)dx, \quad v_1,v_2\in\mathscr{V}, \quad (8)$$

with $L_{\mathscr{V}}$ being a positive definite, self-adjoint, differential operator, analogous definition holds for $\langle\cdot,\cdot\rangle_{\mathscr{W}}$. For the case of the space of kinematics we choose L^2 inner product

$$\langle k_1,k_2\rangle_V = \int_{R^n} k_1^\top(x)k_2(x)dx, \quad k_i\in V. \quad (9)$$

According to [30], if the vector field u_ϑ is the solution of the problem (5), the Euler-Poincaré reduction may be applied to simplify the problem to the following one

$$\min_{P_0} E(P_0) = \frac{1}{2}\|u_0(P_0)\|^2_{\mathscr{V}\times\mathscr{W}} + \frac{1}{2\sigma^2}\|k_1-k\|^2_V, \quad (10)$$

subject to

$$\begin{cases} \frac{\partial k_\vartheta}{\partial\vartheta} = w_\vartheta(k_\vartheta) - Dk_\vartheta\cdot v_\vartheta, \\ \frac{\partial P_\vartheta}{\partial\vartheta} = -(Dw_\vartheta(k_\vartheta))^\top P_\vartheta - \mathrm{div}(P_\vartheta v_\vartheta^\top), \\ L_{\mathscr{V}}v_\vartheta = Dk_\vartheta^\top P_\vartheta, \\ L_{\mathscr{W}}w_\vartheta = P_\vartheta, \end{cases} \quad (11)$$

where k_1 is defined as the solution of the system of equations, D is a differential operator with respect to the spatial argument of a mapping, i.e., $Dk(x) = \partial_x k(x)$, and div denotes the divergence operator, for rank-2 tensor $A = A(x)$, $f = \mathrm{div}(A)$, results in $f_j = \sum_i \frac{\partial A^{ij}}{\partial x_i}$. The differential equations (11) are the evolution equations on the cotangent bundle T^*V of the kinematics space V.

In fact, the problem stated above is a two-point boundary value problem and may be rephrased as follows: find the initial momenta P_0, such that the system of differential equations from above satisfies $k_{t=0} = k_0$ and

$$P_1 + \frac{\partial}{\partial k_1}\frac{1}{2\sigma^2}\|k_1-k\|^2_V = 0. \quad (12)$$

A common approach is solving of such a problem with the shooting method employing the adjoint equations or just with the appropriate numerical optimisation methods.

The solution to the optimization problem (10) solves our calibration problem. Indeed, starting with the nominal kinematics and the optimal initial momenta we can evolve the nominal kinematics to the actual one through the equations (11). The main pitfall of such a formulation is that we have to provide actual kinematics to calculate the value of the cost functional for each step of the optimisation process. Unfortunately, the actual kinematics is not known and we would like to retrive that model. What we are sure about the actual kinematics is that it is available to us only by a finite number of measurements. Due to that, we shall consider the relaxed problem, which we will do in the following section.

4. IMPLEMENTATION

As we pointed out in the previous section, the actual kinematics is not available to us in terms of mapping. We are able to sample the kinematics by taking the measurements at certain points in the internal and external space. This observation pushes us to consider the relaxed problem that takes into account this inconvenience. Keeping this in mind, let us formalise the notion of measurements.

The robot's nominal kinematics (kinematics model) k_0 is given as a map (3) and we assume that we get this relation, e.g., by a standard Denavit-Hartenberg algorithm. Let k be the kinematics of the actual robot – the one we are looking for. We expect that k is available to us only by measurements. From a practical viewpoint, the measurements are treated as the collections of N pairs of the joint positions and their corresponding end-effector positions. We denote them as $x = (x_1,\ldots,x_N)$, $x_i\in R^n$ and $y = \big(k(x_1),\ldots,k(x_N)\big) = (y_1,\ldots,y_N)$, $y_i\in R^m$, respectively. So having these collections of measurements x and y, the goal is to find diffeomorphisms ψ and φ transforming the nominal kinematics that resembles the real one, i.e.

$$\psi\circ k_0\circ\varphi^{-1} = k. \quad (13)$$

Formulating the energy functional in relaxed manner involves considering the error between nominal and actual kinematics at specific measurement points, rather than across the entire domain. Yet, despite this adjustment, the problem remains infinite-dimensional, requiring a numerical solution. By utilising reproducing kernels from Reproducing Kernel Hilbert Spaces to parameterise vector fields, we can overcome the technical hurdles previously encountered. This widely accepted approach immerses the problem into an RKHS [29], effectively reducing the problem from an infinite-dimensional to a finite-dimensional one based on the number of measurements taken. According to the Moore-Aronszajn theorem (see, e.g, [31]), every correctly defined kernel K simultaneously defines a corresponding RKHS. So, by a proper kernel choice, we select an adequate RKHS that enforces appropriate smoothness on vector fields. On the other hand this mapping can be built directly from the bijective and self-adjoint differential operators, [29], in such a case, for the differential operator L the reproducing kernel K is the inverse of that operator $K = L^{-1}$. Looking closely at the spaces of the vector fields $\mathscr{V}$ and $\mathscr{W}$ both are Hilbert spaces equipped with the inner products and

differential operators $L_{\mathscr{V}}, L_{\mathscr{W}}$ being the dual operators at the same time. So, from now on, we assume that the vector fields $v_\vartheta \in \mathscr{V}$ and $w_\vartheta \in \mathscr{W}$ belong to a proper RKHS, $\mathscr{V}$ or $\mathscr{W}$, with the kernels $K_{\mathscr{V}}, K_{\mathscr{W}}$ corresponding to the operators $L_{\mathscr{V}}, L_{\mathscr{W}}$. According to the [32], if one's choice of the differential operator is

$$L = \sum_{\beta \in \mathbb{N}_0^n} \frac{1}{2^{|\beta|} \prod_{j=1}^n (\beta_j)} D^{2\beta},$$

the corresponding kernel is the widely used Gauss kernel

$$K(x,y) = (2\pi)^{-\frac{n}{2}} e^{-\frac{\|x-y\|}{2}}, \quad x,y \in \mathbb{R}^n.$$

The RKHS distinguishes itself from Hilbert space in that it possesses a reproducing kernel. It admits us to interpolate the vector fields (4) in an arbitrary location based on

$$\begin{aligned} v_\vartheta(x) &= \int_X K_V(x,\xi)\alpha(\vartheta,\xi)\,\mathrm{d}\xi, \quad \text{for } \alpha(\vartheta,\xi) \in R^m, \\ w_\vartheta(y) &= \int_Y K_W(y,\eta)\beta(\vartheta,\eta)\,\mathrm{d}\eta, \quad \text{for } \beta(\vartheta,\eta) \in R^m, \end{aligned} \tag{14}$$

where $K_{\mathscr{V}}(x,\xi)$ and $K_{\mathscr{W}}(y,\eta)$ denotes the reproducing kernels for $\mathscr{V}$ and $\mathscr{W}$, and $\alpha(\vartheta,\xi)$ and $\beta(\vartheta,\eta)$ are vectors in R^m coming from the construction of the reproducing kernels for the spaces consisting of multi-dimensional vector fields (more detailed explanation in [29]), they may be interpreted as a sort of suitable weighting coefficients

$$\begin{aligned} v_\vartheta(x) &= \sum_{i=1}^N K_{\mathscr{V}}(x,\xi_i)\alpha_i(\vartheta), \\ w_\vartheta(y) &= \sum_{i=1}^N K_{\mathscr{W}}(y,\eta_i)\beta_i(\vartheta). \end{aligned} \tag{15}$$

Keeping that in mind, we formulate the relaxed calibration by diffeomorphisms as follows. For given nominal kinematics k_0 and the measurements $(x_i, y_i), i = 1,\ldots,N$ taken from the actual kinematics k $(k, k_0 \in V)$, find $P_0 \in V^*$ that minimises

$$\begin{aligned} E(P_0) = &\frac{1}{2}\sum_{i,j=1}^N P_0^\top(x_i) Dk_0(x_i) K_{\mathscr{V}}(x_i,x_j) Dk_0(x_j)^\top P_0(x_j) \\ &+ \frac{1}{2}\sum_{i,j=1}^N P_0^\top(x_i) K_{\mathscr{W}}(k_0(x_i),k_0(x_j)) P_0(x_j) \\ &+ \frac{1}{2\sigma^2}\sum_{i=1}^N \|k_1(x_i) - y_i\|_2^2, \end{aligned} \tag{16}$$

where $k_1(x_i)$ is defined as the solution of the system of equations

$$\begin{cases} \frac{\partial k_\vartheta(x_i)}{\partial \vartheta} = w_\vartheta(k_\vartheta(x_i)) - Dk_\vartheta(x_i)\cdot v_\vartheta(x_i), \\ \frac{\partial P_\vartheta^i}{\partial \vartheta} = -(Dw_\vartheta(k_\vartheta(x_i)))^\top P_\vartheta^i - \mathrm{div}(P_\vartheta^i v_\vartheta^\top(x_i)), \\ v_\vartheta(x_i) = \sum_j^N K_{\mathscr{V}}(x_i,x_j) Dk_\vartheta(x_j)^\top P_\vartheta^j, \\ w_\vartheta(y_i) = \sum_j^N K_{\mathscr{W}}(y_i,y_j) P_\vartheta^j, \end{cases} \tag{17}$$

evaluated at the point $t = 1$.

One should notice that the Jacobian of the current kinematics k_ϑ is needed at every evaluation of the differential equation. Unfortunately, we cannot compute it analytically. Instead, let us look at the evolution of that Jacobian along the evolution curve. It is easy to check that $Dk_\vartheta = D\psi_\vartheta Dk_0 D\varphi_\vartheta^{-1}$ is a solution to the following differential equation

$$\frac{\partial Dk_\vartheta}{\partial \vartheta} = Dw_\vartheta(k_\vartheta) Dk_\vartheta - Dk_\vartheta Dv_\vartheta \tag{18}$$

being a type of Sylvester differential equation. Evaluation of (18) for a certain point x_i yields

$$\frac{\partial Dk(x_i)}{\partial \vartheta} = Dw_\vartheta(k_\vartheta(x_i)) Dk_\vartheta(x_i) - Dk_\vartheta(x_i) Dv_\vartheta(x_i). \tag{19}$$

Thus, supplementing the set of equations (17) with (19) is sufficient to find the initial momenta P_0 using on of the numerical optimisation procedure. We need to look for P_0 once per robot and a data set of measurements (once per calibration process). Once the solution we can compute the actual kinematics, namely the relation between task space variables y, and an arbitrary value of joint variables ξ, with the following

$$\begin{cases} \frac{\partial k_\vartheta(\xi)}{\partial \vartheta} = w_\vartheta(k_\vartheta(\xi)) - Dk_\vartheta(\xi)\cdot v_\vartheta(\xi), \\ \frac{\partial Dk(\xi)}{dt} = Dw(k_\vartheta(\xi)) Dk_\vartheta(\xi) - Dk_\vartheta(\xi) Dv(\xi), \\ v_\vartheta(\xi) = \sum_j^N K_{\mathscr{V}}(\xi,x_j) Dk_\vartheta(x_j)^\top P_\vartheta^j, \\ w_\vartheta(k_\vartheta(\xi)) = \sum_j^N K_{\mathscr{W}}(k_\vartheta(\xi)),k_\vartheta(x_j)) P_\vartheta^j, \end{cases} \tag{20}$$

where P_ϑ^i and $k_\vartheta(x_i)$ can be obtained and reused from the solution of the previous system of equations for the measurement points x_i. Finally, the kinematics relation is given by

$$y = k_1(\xi), \tag{21}$$

where $k_1(\xi)$ is a value of a resultant trajectory $k_\vartheta(\xi)$ of (20) at point $\vartheta = 1$ for a given configuration ξ. The presented calibration may be outlined as, from our calibration process (offline) we at least determine the vector fields $v_\vartheta(x)$ and $w_\vartheta(y)$ and may interpret them with corresponding kernel $K_{\mathscr{V}}$ and $K_{\mathscr{W}}$. So the solution, the actual kinematics k_1 is the value of the trajectory k_ϑ of (20) in point $\vartheta = 1$. The idea behind the first equation in (20) is depicted in Fig. 1. As can be seen, as the ϑ increases, the mapping $k_\vartheta(x_i)$, continuously maps a point x_i from the internal space X into a point $k_\vartheta(x_i)$ in the external space Y. For $\vartheta = 0$, we arrive at the point resulting from nominal kinematics, and for $\vartheta = 1$ the computation yields with the point $k_1(x_i)$ (calibrated kinematics) which coincides, as expected, with the measurements. By utilizing the concept of reproducing kernels, we can similarly determine the outcome of calibrated kinematics for any point that does not align with the measurement using (20).

The computational flow of the entire calibration procedure is illustrated in Fig. 2 for clarity, while the pseudocode for the algorithm is provided in Listings 1 and 2.

Summarising the introduced approach and applying it into a classical calibration procedure, we follow four steps outlined in [2]. Firstly, we start with a first-guess model of nominal kinematics (3). It can be a standard model attained through the Denavit-Hartenberg algorithm. There is no requirement to consider some prior knowledge of phenomena different from kinematics (bends, joint compliance, etc.). In the second step, we collect N independent pairs of (x,y) measurements configuration and the corresponding pose of the end-effector. The

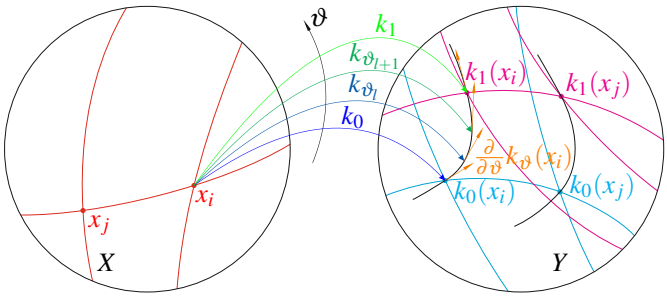

Fig. 1. Actual kinematics computation.

Algorithm 1 LR calibration, offline part

Require:
$X=(x_1,\ldots,x_N), Y=(k_r(x_1),\ldots,k_r(x_N))$ ▷ *Sets of N measurements of configurations and corresponding end-effector poses,*
$k, K_{\mathscr{V}}, K_{\mathscr{W}}, \sigma$ ▷ *Nominal kinematics, reproducing kernels for $\mathscr{V}$ and $\mathscr{W}$ spaces, regularization coefficient,*
$\mu, \varepsilon, max\_iter$ ▷ *step size, optimization tolerance, number of iterations*
function LR_CALIBRATION($X, Y, k, K_{\mathscr{V}}, K_{\mathscr{W}}, \sigma, \varepsilon, max\_iter$)
  Initialize $P_0 = (P_0^1,\ldots,P_0^N) \leftarrow 0$
  Set iteration counter $k \leftarrow 0$
  while $i <$ max_iter **do**
    Solve ODEs (17) along $\vartheta \in (0,1)$
    Compute gradient of (12), i.e., ∇_{P_0}
    if $\|\nabla_{P_0}\| < \varepsilon$ **then**
      break ▷ *Convergence criteria met*
    end if
    Update the momenta $P_0 \leftarrow P_0 - \mu\nabla_{P_0}$
    Increment iteration counter $i \leftarrow i+1$
  end while
  return $(X, P_0, k, K_{\mathscr{V}}, K_{\mathscr{W}})$ ▷ *Tuple encoding the calibrated kinematics*
end function

Algorithm 2 LR calibration, online part

Require:
ξ ▷ *Point for evaluation of the calibrated kinematics*
$(X, P_0, k, K_{\mathscr{V}}, K_{\mathscr{W}})$ ▷ *Tuple encoding the calibrated kinematics, returned from the offline part*

function EVALUATE($\xi, X, P_0, k, K_{\mathscr{V}}, K_{\mathscr{W}}$)
  Solve ODEs (20) with (16) along $\vartheta \in (0,1)$
  return $(k_1(\xi), Dk_1(\xi))$ ▷ *Calibrated kinematics and its Jacobian at given point ξ, obtained as the endpoint value of (20)*
end function

third step involves a reformulation of the identification procedure to the introduced one that based on diffeomorphic deformation (13), contrary to the original approach proposed in [2, 1, 3] and many others. This reformulation leads us to LDDMM and to the dynamical system driving the calibration process that can be numerically solved with given initial conditions. Finally, the last calibration step, the implementation, can be achieved through equation (21).

5. SIMULATION RESULTS

The efficiency of the Calibration by Diffeomorphisms, presented in previous sections, will be evaluated through simulation results. We have chosen an *RR* manipulator as our simulational testbed to accomplish that. The schematic diagram of the selected robot has been depicted in Fig. 3. The values of the link lengths in the considered robot are set to $l_1 = 1$ and $l_2 = 0.5$, whilst the nominal kinematics model of an *RR* robot has been obtained via the standard Denavit-Hartenberg procedure. Thus, the kinematics in coordinates takes the form

$$\begin{pmatrix} y_1 \\ y_2 \end{pmatrix} = \begin{pmatrix} l_1\cos(x_1) + l_2\cos(x_1+x_2) \\ l_1\sin(x_1) + l_2\sin(x_1+x_2) \end{pmatrix}, \tag{22}$$

where $y = (y_1, y_2) \in R^2$ is a vector in task space representing the position of the end-effector, and $x = (x_1, x_2) \in T^2 \simeq R^2$ denotes a joint space vector collecting angles of a first and second joint respectively (see Fig. 3).

To perform the robot calibration, we need to generate a dataset of measurements, namely the pairs (x_i, y_{r_i}) for $i = 1,\ldots,N$ of a real robot joint positions x_i corresponding with the end-effector positions y_{r_i}. For this reason, we introduce new kinematics reflecting the actual manipulator kinematics. The desired (real) kinematic relationship is expressed by

$$y_r = k_r(x), \tag{23}$$

which we design according to the elastostatic model proposed in [33], with additional discrepancies introduced in link lengths and robot base position. We assume this relationship is unknown and remains hidden during the calibration process. It serves only as a measurement source and a benchmark for the result assessment. We will refer to the relationship (23) as the desired (real) kinematics, as opposed to the actual kinematics delivered from the calibration algorithm.

In the real manipulator kinematics (23), we have introduced three types of disturbances. Firstly we changed the link lengths by around 10%. Secondly, we add an offset of the base mounting point location, that could be interpreted as a misaligned base coordinate system. Finally, the third disturbance involved bending, stretching, and shrinking of the links. We assume that the links of the manipulator can bend according to the influence of gravity. One should notice that we deal only with the static kinematics model. So the robot acceleration is not considered and does not affect link bending. It is easy to imagine that the end-effector position can vary significantly depending on the elasticity parameter.

To calibrate the manipulator based on the introduced theory, we need an initial kinematics relation as a starting point. It is helpful to compare the real (unknown) kinematics to the initial one. Figure 4 shows the comparison presenting the position of the end-effector of the nominal manipulator and the real one at a few configurations – the same for each manipulator. One can notice from Figure 4 that discrepancies in the end-effector

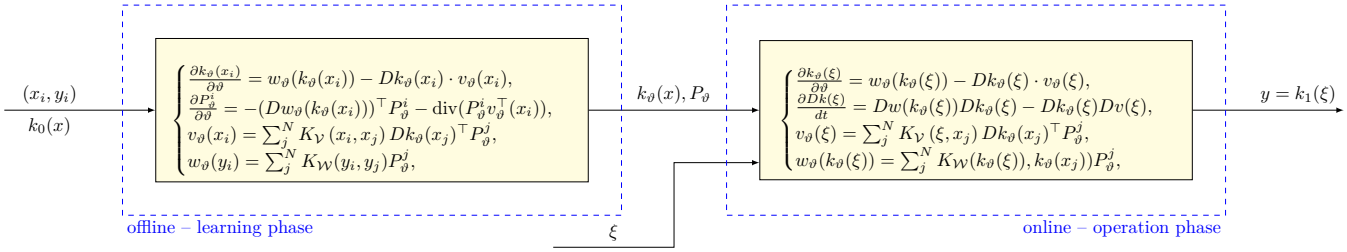

Fig. 2. Computation flow of the Calibration by Diffeomorphisms.

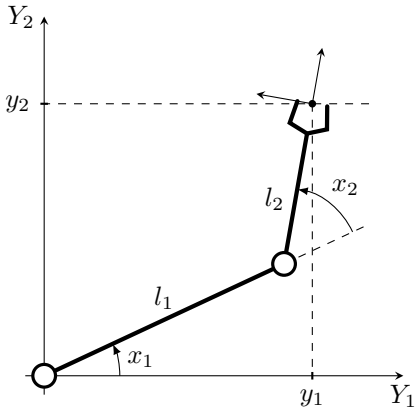

Fig. 3. Schematic diagram of the *RR* manipulator.

position can be relatively considerable and, according to introduced disturbances, can vary along the workspace.

Having our testbed established, we can specify the Calibration by diffeomorphism problem to the RR manipulator case. Fig. 5 presents a specific instance of a diagram (1) for our testbed (*RR* manipulator). Now we can show the topologies of the corresponding spaces X (inner space) and Y (external space). While our model is an *RR* manipulator, the inner (joint) space is a torus T^2. The external (task) space is a subspace of an R^2 and depends on the link lengths. In the presented scenario, the manipulator work range forms an annulus. Also, we

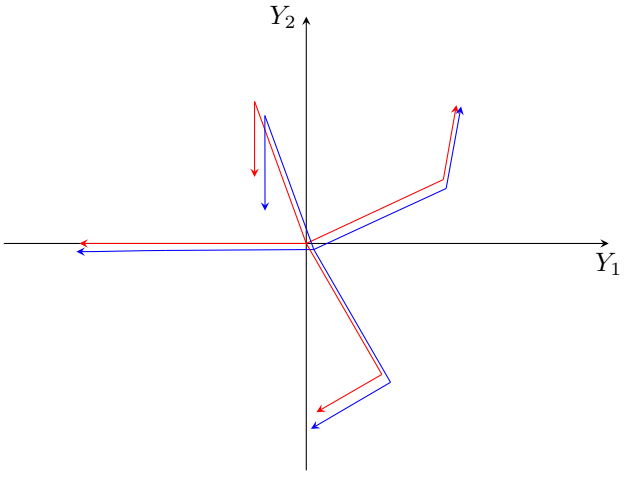

Fig. 4. The initial and the real manipulator poses comparison.

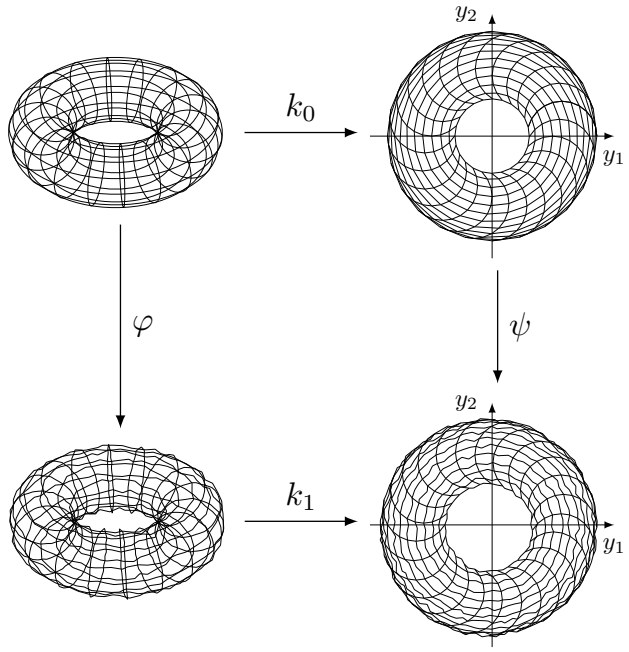

Fig. 5. Calibration by diffeomorphism for *RR* manipulator.

may observe the influence of the resultant diffeomorphisms. The effect of the φ diffeomorphism is to distort, in a proper way, the geometry of the x space while preserving its topology and differential structure. Analogously, the diffeomorphism ψ transforms diffeomorphically the y space. After such transformation, the proper composition of diffeomorphisms with the initial kinematics k_0 as in (13) produces the sought relation of actual kinematics k_1.

Proceeding to the simulational part, we have to find initial momenta P^i_0 such that its value, under the evolution through the equation, at time $t = 1$ satisfy the boundary constraint $P^i_1 = -\frac{\partial}{\partial k_1(x_i)} \frac{1}{2\sigma^2} \|k_1(x_i) - k_2(x_i)\|^2_2$. Further, we obtain the actual kinematics by (21) under (20). We perform the computation by the *Matlab* built-in algebraic and differential equation solvers using the *Kernel Operations (KeOps)* library [34], supplying *Matlab* with functions for efficient calculations of kernel-related operations. The library allows one for easy computation on GPU. Nonetheless, we have not used yet those capabilities in the simulations. As kernel functions, we chose a Gaussian kernel and a positive kernel properly defined on the torus, [35]. Thus, $K_{\mathscr{W}} = \exp\left(-\frac{|x-y|^2}{a}\right)$ and

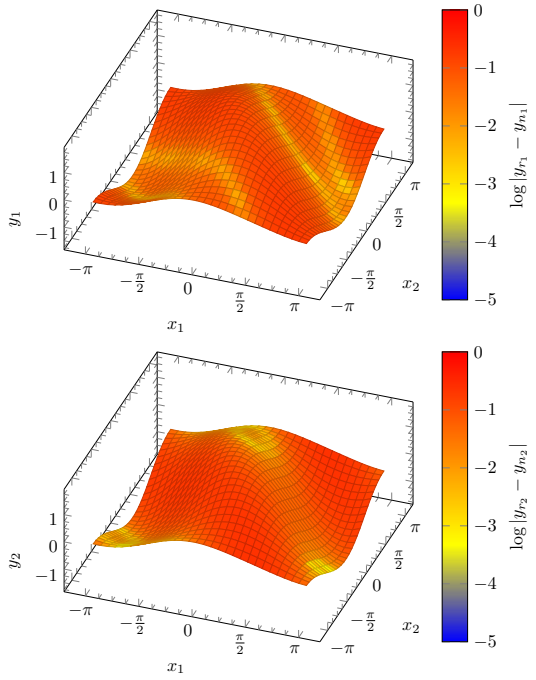

Fig. 6. The real versus nominal kinematics.

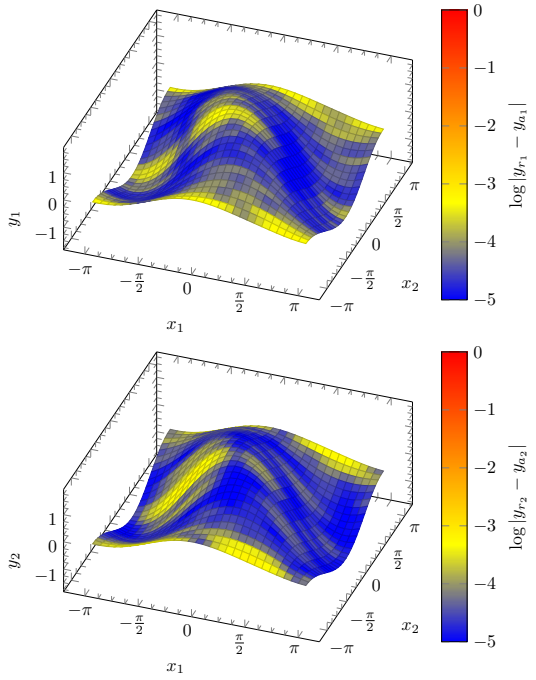

Fig. 7. The real versus actual kinematics.

$K_{\mathscr{Y}} = \gamma \exp\left(b_1(\cos(x_i - y_i) - 1) + b_2(\cos(x_2 - y_2) - 1)\right)$. The value of the parameters for $K_{\mathscr{Y}}$ have been set to $b_1 = 1.0186$, $b_2 = 1.0186$, whereas for $K_{\mathscr{W}} = K(x,y)$ to $a = 1.0270$. The role of the weight parameter γ in the $K_{\mathscr{Y}}$ kernel is to enforce the preference between the φ and ψ diffeomorphisms and in the simulation took the value $\gamma = 8$, the regularization parameter $\sigma = 100$. The real kinematics have been sampled with 256 measurements taken from a grid defined on configurational space.

The simulation results of the whole calibration process are depicted in Figures 6–12. For comparison purposes, each figure demonstrates the state before and after calibration concerning the desired one in both cases.

Plots in Figure 6 visualise the uncalibrated kinematics. The surfaces represent the real kinematics expressed by (23), and the colour maps the logarithm of absolute value of the discrepancy between (23) and the nominal (22) kinematics. One can notice that we start from relatively large errors that are mostly around 0.1 to 0.15 length units.

Contrary to the Figure 6, figure 7 depict the actual (final) kinematics acquired from our method. Once again, the surface presents the respective y_1 and y_2 components of the real kinematics (23), while this time, the colour indicates the resultant errors $\log|y_{r_i} - y_{a_i}|$ along each task space coordinate. It may be concluded from the collection of figures 6–7 that our method reduces the discrepancy between the actual and the real kinematics by 4-5 orders of magnitude.

Figures 8 and 9 provide us with another comparative analysis. This time, we draw a whole workspace of the *RR* manipulator by sweeping the two joint variables on the full range. In both Figures, the red mesh represents the real (desired) kinematics, while the blue one indicates nominal or actual kinematics – respectively to the Figures. The calibration error becomes

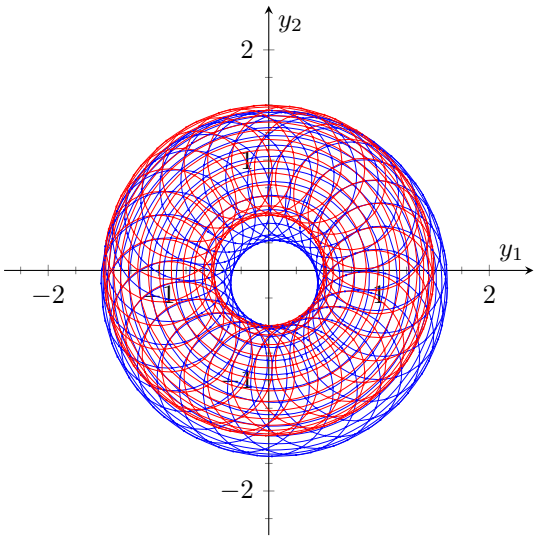

Fig. 8. The grid in workspace comparison between k_r and k_n.

lower when the two task space grids coincide. One can observe that the grid generated with the actual kinematics (Figure 9) is closer to the desired (real) one than the nominal grid presented in Figure 8. Since the already presented simulational results have been prepared for the regular grid of joint variables and may not be objective enough, we have performed other simulations for randomly drawn configurations. Upon that, we drew a set of 3000 uniformly distributed samples of joint variables and determined their corresponding task space values. We are going to discuss the results in both qualitative and quantitative manner.

Let us start with the qualitative analysis. Figures 10 and 11 present the heatmap of calibration error distribution in the

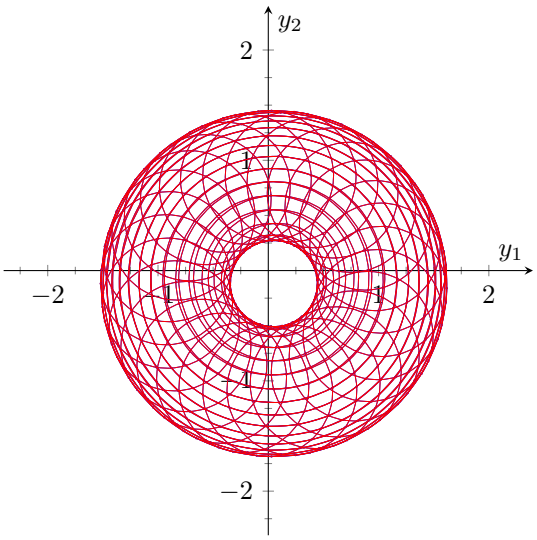

Fig. 9. The grid in workspace comparison between k_r and k_a.

workspace. As in the previous Figures, they exhibit errors before and after the calibration procedure, i.e., for the initial (nominal) and final (actual) kinematics.

Please keep in mind that the colour still is in the logarithm scale for convenience, and once again, one should notice that we reduce the error by more than three orders of magnitude. It is also worth noting that we achieve slightly higher error values at the border of the workspace when the manipulator is in its singular position.

Quantitative analysis can be performed with the help of histograms in Figure 12. These histograms indicate that the average error value has shifted significantly after calibration by at least three orders of magnitude.

Summarizing, the simulation results demonstrate that our innovative method for calibration of robot kinematics is an effective way to achieve a more accurate kinematics relationship.

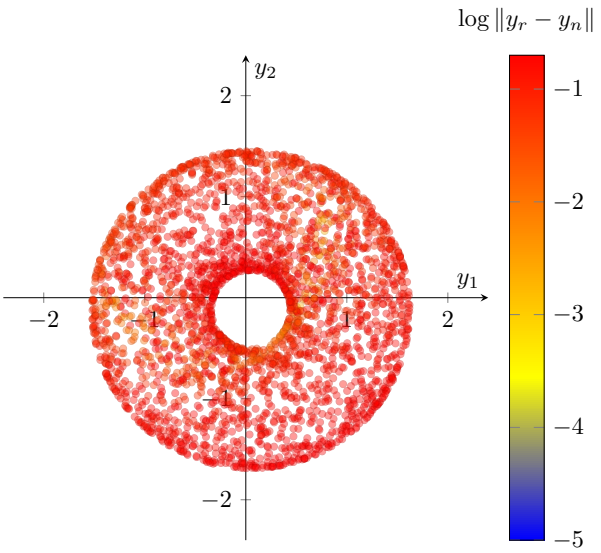

Fig. 10. Calibration error $\|y_r - y_n\|$ heatmap.

The accuracy of the presented results can be further improved by increasing the computation precision and taking a more extensive set of measurement points.

We are conscious of the computational aspects of the proposed solution. The most time demanding part is to solve a system of equations (17), which takes around 470 second on the 12 core, 3.8 GHz CPU processor. Considering that the system of equations (17) is solved only once, the result is remarkable.

We are aware that the efficiency of the presented calibration method is confirmed simulatively only. One of our future goals is to establish the experimental stand. However, this task is quite challenging, particularly on the mechanical part, since our approach can deal with a large spectrum of discrepancies, even the unpredictive ones, so it is hard to design and build the hardware that will be able to imitate the selected phenomenon in a desired way. Nevertheless, we look to perform experi-

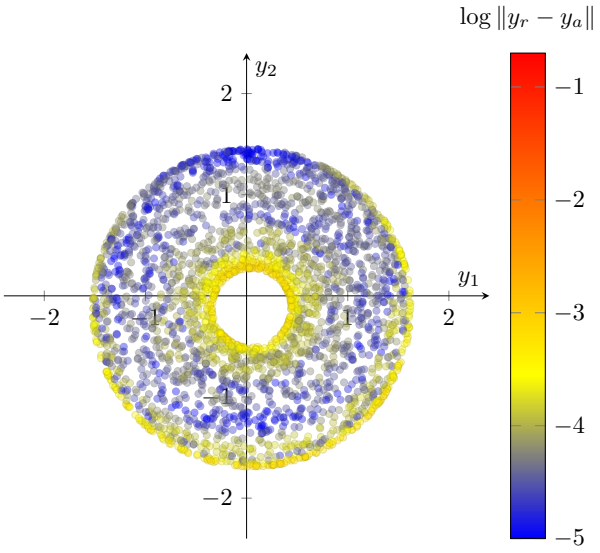

Fig. 11. Calibration error $\|y_r - y_a\|$ heatmap.

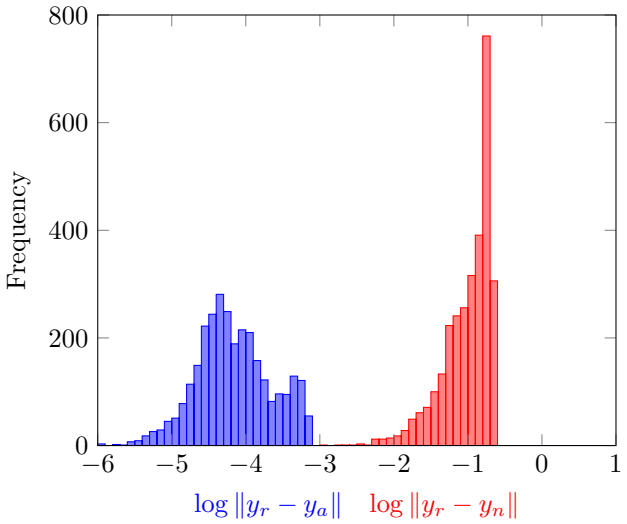

Fig. 12. Frequency of occurrence of values of $\|y_r - y_a\|$ and $\|y_r - y_n\|$.

ments in the future.

6. CONCLUSIONS

Based on the presented content, it can be concluded that the proposed approach to robot calibration has effectively solved the stated problem. Therefore, one may consider our method of Calibration by Diffeomorphisms as a promising utility for robot kinematics calibration or even for a broader class of model identification problems, specifically when the source of the discrepancies is unknown or hard to model. The efficiency of the presented approach has been depicted with simulation results. Moreover, it is possible to further enhance the method's accuracy simply by using more measured data and calculating the diffeomorphisms accordingly.

It is important to emphasize that the presented approach of Calibration by Diffeomorphisms requires the same level (or even less) of prior knowledge as the classical approach. The reference model it works with, can be the first-guess model, for example, one determined with a Denavit-Hartenberg procedure. Forasmuch as it is relatively challenging to discover and model the existing phenomena that influence the discrepancies between the kinematics relation and reality, the introduced method may be a remedy for that. Worth mentioning is that the methodology combines theoretical and empirical approaches. It seems to be well-balanced between exact modeling and inferring model from data, preserving essential properties of the robot kinematics, i.e. topological and differential structure. Nonetheless, for the sake of the infancy of the presented method, there are still research issues to address that we would like to spell out and, what follows, highlight our future research goals.

- In the current state, the method works with kinematics expressed in the coordinates; hence the problem arises when we deal with kinematics taking values in the SE(3) or the other space with geometric structures different from Euclidean. To overcome that, we should generalize the approach considering these cases. An optimistic perspective for solving the problem is given by the research [36] focusing, among others, on designing stable vector fields on the Lie groups. It is expected that some of their ideas may be successfully incorporated into Calibration by Diffeomorphisms.
- Another urgent issue to consider is to investigate how to increase the accuracy and computational efficiency of the algorithm. Specifically, increasing the dimensions of the task and joint space or the accuracy of the solution inevitably demands more measurement samples, which drives us to the curse of dimensionality. One of the enhancements is to use GPUs for computational purposes. This path seems to be a symptomatic solution and relatively easy to implement. More fruitful appear to reformulate or simplify the problem by introducing constraints, for example, on the vector fields.
- A distinct area of investigation is reproducing kernel functions. Currently used Gaussian kernels pretend to be a reasonable first choice because they allow us to reproduce the vector fields with a demanded degree of smoothness; however, it is worth considering alternate functions to already used ones. It would be tremendous to answer the question of what kernel function should be used in robotics applications. Other kernel-related issues to solve concern the parameters and procedure of choosing their values. For now, their values are determined based on the researcher's experience. A suitable objective method would simplify the usage.
- A selection of the measurement points offers some opportunity for exploration as well. It should be worth determining how the number of measurement and their distribution in the joint/task space influence the accuracy and computation time. Simply speaking, we should find the answer to the question: How should the measurements be taken to improve the accuracy and computation time? We expect some clues for this issue may be found in [37].
- An innovative and promising idea is to leverage introduced methods and diffeomorphometry along with its metric studies of shapes to develop a holistic framework for the predictive maintenance of robots and machines.
- Last but not least is the approach validation by physical experiment with a real manipulator. As has been mentioned, the most challenging part is to design and build the hardware that allows for the introduction of the phenomena in a controlled way and makes it possible to test our method against them.

REFERENCES

[1] B. Siciliano and O. Khatib, *Springer Handbook of Robotics*. Berlin, Heidelberg: Springer-Verlag, 2007.
[2] Z. Roth, B. Mooring, and B. Ravani, "An Overview of Robot Calibration," *IEEE Journal on Robotics and Automation*, vol. 3, no. 5, pp. 377–385, 1987.
[3] W. Khalil and E. Dombre, *Modeling, Identification and Control of Robots*. Taylor & Francis, 2002.
[4] G. Zhao, P. Zhang, G. Ma, and W. Xiao, "System identification of the nonlinear residual errors of an industrial robot using massive measurements," *Robotics and Computer-Integrated Manufacturing*, vol. 59, pp. 104–114, 2019.
[5] H.-N. Nguyen, J. Zhou, and H.-J. Kang, "A calibration method for enhancing robot accuracy through integration of an extended kalman filter algorithm and an artificial neural network," *Neurocomputing*, vol. 151, pp. 996–1005, 2015.
[6] S. Gadringer, H. Gattringer, A. Müller, and R. Naderer, "Robot Calibration combining Kinematic Model and Neural Network for enhanced Positioning and Orientation Accuracy," *IFAC-PapersOnLine*, vol. 53, no. 2, pp. 8432–8437, 2020.
[7] X. Zhong, J. Lewis, and F. L. N-Nagy, "Inverse robot calibration using artificial neural networks," *Engineering Applications of Artificial Intelligence*, vol. 9, no. 1, pp. 83–93, 1996.
[8] K. Tchoń, "Calibration of Manipulator Kinematics: a Singularity Theory Approach," *IEEE Transactions on*

Robotics and Automation, vol. 8, no. 5, pp. 671–678, 1992.

[9] W. Khalil, M. Gautier, and C. Enguehard, "Identifiable Parameters and Optimum Configurations for Robots Calibration," *Robotica*, vol. 9, no. 1, pp. 63–70, Jan. 1991.

[10] H. Zhuang and Z. Roth, "A Linear Solution to the Kinematic Parameter Identification of Robot Manipulators," *IEEE Transactions on Robotics and Automation*, vol. 9, no. 2, pp. 174–185, Apr. 1993.

[11] M. Abderrahim, A. Khamis, S. Garrido, and L. Moreno, "Accuracy and Calibration Issues of Industrial Manipulators," in *Industrial Robotics: Programming, Simulation and Applications*, L. Kin, Ed. Pro Literatur Verlag, Germany / ARS, Austria, Dec. 2006.

[12] L. Ma, P. Bazzoli, P. M. Sammons, R. G. Landers, and D. A. Bristow, "Modeling and Calibration of High-Order Joint-Dependent Kinematic Errors for Industrial Robots," *Robotics and Computer-Integrated Manufacturing*, vol. 50, pp. 153–167, Apr. 2018.

[13] T. Messay, R. Ordóñez, and E. Marcil, "Computationally Efficient and Robust Kinematic Calibration Methodologies and Their Application to Industrial Robots," *Robotics and Computer-Integrated Manufacturing*, vol. 37, pp. 33–48, Feb. 2016.

[14] M. Dehghani, R. A. McKenzie, R. A. Irani, and M. Ahmadi, "Robot-Mounted Sensing and Local Calibration for High-Accuracy manufacturing," *Robotics and Computer-Integrated Manufacturing*, vol. 79, p. 102429, Feb. 2023.

[15] C. Lightcap, S. Hamner, T. Schmitz, and S. Banks, "Improved Positioning Accuracy of the PA10-6CE Robot with Geometric and Flexibility Calibration," *IEEE Transactions on Robotics*, vol. 24, no. 2, pp. 452–456, Apr. 2008.

[16] J. H. Jang, S. H. Kim, and Y. K. Kwak, "Calibration of Geometric and Non-Geometric Errors of an Industrial Robot," *Robotica*, vol. 19, no. 3, pp. 311–321, May 2001.

[17] Y. Song, M. Liu, B. Lian, Y. Qi, Y. Wang, J. Wu, and Q. Li, "Industrial Serial Robot Calibration Considering Geometric and Deformation Errors," *Robotics and Computer-Integrated Manufacturing*, vol. 76, p. 102328, Aug. 2022.

[18] A. Alamdar, P. Samandi, S. Hanifeh, P. Kheradmand, A. Mirbagheri, F. Farahmand, and S. Sarkar, "Investigation of a Hybrid Kinematic Calibration Method for the Sina Surgical Robot," *IEEE Robotics and Automation Letters*, vol. 5, no. 4, pp. 5276–5282, Oct. 2020.

[19] J. Chen, F. Xie, X.-J. Liu, and Z. Chong, "Elasto-geometrical Calibration of a Hybrid Mobile Robot Considering Gravity Deformation and Stiffness Parameter Errors," *Robotics and Computer-Integrated Manufacturing*, vol. 79, p. 102437, Feb. 2023.

[20] K. Deng, D. Gao, S. Ma, C. Zhao, and Y. Lu, "Elasto-geometrical Error and Gravity Model Calibration of an Industrial Robot Using the Same Optimized Configuration Set," *Robotics and Computer-Integrated Manufacturing*, vol. 83, p. 102558, Oct. 2023.

[21] L. Miao, Y. Zhang, Z. Song, Y. Guo, W. Zhu, and Y. Ke, "A Two-Step Method for Kinematic Parameters Calibration Based on Complete Pose MeasurementVerification on a Heavy-Duty Robot," *Robotics and Computer-Integrated Manufacturing*, vol. 83, p. 102550, Oct. 2023.

[22] J. Santolaria and M. Ginés, "Uncertainty Estimation in Robot Kinematic Calibration," *Robotics and Computer-Integrated Manufacturing*, vol. 29, pp. 370–384, Apr. 2013.

[23] R. He, X. Li, T. Shi, B. Wu, Y. Zhao, F. Han, S. Yang, S. Huang, and S. Yang, "A Kinematic Calibration Method Based on the Product of Exponentials Formula for Serial Robot Using Position Measurements," *Robotica*, vol. 33, no. 6, pp. 1295–1313, Jul. 2015.

[24] T. Sun, B. Lian, S. Yang, and Y. Song, "Kinematic Calibration of Serial and Parallel Robots Based on Finite and Instantaneous Screw Theory," *IEEE Transactions on Robotics*, vol. 36, no. 3, pp. 816–834, Jun. 2020.

[25] H. M. Balanji, A. E. Turgut, and L. T. Tunc, "A Novel Vision-Based Calibration Framework for Industrial Robotic Manipulators," *Robotics and Computer-Integrated Manufacturing*, vol. 73, p. 102248, Feb. 2022.

[26] R. Orozco and A. Ratajczak, "Image Registration and Calibration of Manipulator Kinematics," in *Postępy robotyki*, A. Mazur and C. Zieliński, Eds. Oficyna Wydawnicza Politechniki Warszawskiej, 2022, pp. 21–30, in Polish.

[27] M. F. Beg, M. Miller, A. Trouvé, and L. Younes, "Computing Large Deformation Metric Mappings via Geodesic Flows of Diffeomorphisms," *International Journal of Computer Vision*, vol. 61, pp. 139–157, Feb. 2005.

[28] M. Golubitsky and V. Guillemin, *Stable Mappings and Their Singularities*, ser. Graduate texts in mathematics. Springer, 1974.

[29] L. Younes, *Shapes and diffeomorphisms*, ser. Applied mathematical sciences. Springer, 2019, vol. 171.

[30] M. Bruveris and D. D. Holm, *Geometry of Image Registration: The Diffeomorphism Group and Momentum Maps*. New York, NY: Springer New York, 2015, pp. 19–56.

[31] S. Saitoh and Y. Sawano, *Theory of reproducing kernels and applications*, 1st ed., ser. Developments in Mathematics. Singapore, Singapore: Springer, Oct. 2016.

[32] E. Novak, M. Ullrich, H. Woniakowski, and S. Zhang, "Reproducing kernels of sobolev spaces on d and applications to embedding constants and tractability," *Analysis and Applications*, vol. 16, no. 05, p. 693715, Aug. 2018.

[33] W. J. Book, "Analysis of Massless Elastic Chains with Servo Controlled Joints," *Journal of Dynamic Systems, Measurement, and Control*, vol. 101, no. 3, pp. 187–192, Sep. 1979.

[34] B. Charlier, J. Feydy, J. A. Glaunès, F.-D. Collin, and G. Durif, "Kernel Operations on the GPU, with Autodiff, without Memory Overflows," *Journal of Machine Learning Research*, vol. 22, no. 74, pp. 1–6, 2021.

[35] F. J. Narcowich, "Generalized hermite interpolation and positive definite kernels on a riemannian manifold," *Jour-*

nal of Mathematical Analysis and Applications, vol. 190, no. 1, pp. 165–193, 1995.

[36] J. Urain, D. Tateo, J. Peters, and J. Jesus, "Learning Stable Vector Fields on Lie Groups," *IEEE Robotics and Automation Letters*, vol. PP, pp. 1–8, Oct. 2022.

[37] H. Wang, T. Gao, J. Kinugawa, and K. Kosuge, "Finding Measurement Configurations for Accurate Robot Calibration: Validation with a Cable-Driven Robot," *IEEE Transactions on Robotics*, vol. 33, no. 5, pp. 1156–1169, Oct. 2017.